Unique mechanistic insights into pathways associated with the synergistic activity of polymyxin B and caspofungin against multidrug-resistant *Klebsiella pneumoniae*

Maytham Hussein [a], Labell J.M. Wong [a], Jinxin Zhao [b], Vanessa E. Rees [d], Rafah Allobawi [a], Rajnikant Sharma [c], Gauri G. Rao [c], Mark Baker [e], Jian Li [b], Tony Velkov [a,*]

[a] *Department of Biochemistry and Pharmacology, School of Biomedical Sciences, Faculty of Medicine, Dentistry and Health Sciences, The University of Melbourne, Parkville, VIC 3010, Australia*
[b] *Monash Biomedicine Discovery Institute, Department of Microbiology, Monash University, Clayton, Victoria 3800, Australia*
[c] *Division of Pharmacotherapy and Experimental Therapeutics, Eshelman School of Pharmacy, University of North Carolina, Chapel Hill, NC, USA*
[d] *The Novo Nordisk Centre for Biosustainability, The Technical University of Denmark (DTU), 2800 Kgs. Lyngby, Denmark*
[e] *Discipline of Biological Sciences, Priority Research Centre in Reproductive Biology, Faculty of Science and IT, University of Newcastle, University Drive, Callaghan, NSW 2308, Australia*

A R T I C L E   I N F O

A B S T R A C T

Klebsiella pneumoniae is an opportunistic Gram-negative pathogen causing nosocomial infections. *K. pneumoniae* rapidly acquires antibiotic resistance and is known as a reservoir for resistance genes. Polymyxins remain effective as a last-line therapy against infections caused by multidrug-resistant (MDR) *K. pneumoniae*; however, resistance to polymyxins emerges rapidly with monotherapy. Synergistic combinations of polymyxins with FDA-approved non-antibiotics are a novel approach to preserve its efficacy whilst minimising the emergence of polymyxin resistance in *K. pneumoniae*. This study aimed to investigate the synergistic antibacterial activity of polymyxin B in combination with the antifungal caspofungin against *K. pneumoniae*. The combination of polymyxin B and caspofungin showed marked synergistic antibacterial killing activity in checkerboard broth microdilution and static time-kill assays at clinically relevant concentrations at early (0.5 and 1 h) and later (4 h) time points. The potential bacterial killing mechanism of the combination was studied against *K. pneumoniae* FADDI-KP001 using metabolomics and transcriptomics studies at 0.5, 1 and 4 h. The key pathways involved in the synergistic killing action of the combination were cell wall assembly (peptidoglycan and lipopolysaccharide biosynthesis), central carbon metabolism (glycolysis, pentose phosphate pathway and tricarboxylic acid cycle) and fatty acid biosynthesis. Moreover, the combination inhibited the most common bacterial virulence pathway (phosphotransferase system) as well as the multi-resistant efflux mechanisms, including ATP-binding cassette (ABC) transporter pathway. Overall, this study sheds light on the possibility of a polymyxin-caspofungin combination for the treatment of infections caused by *K. pneumoniae* and may help repurpose FDA-approved caspofungin against MDR *K. pneumoniae* infections.

© 2022 Published by Elsevier B.V. on behalf of Research Network of Computational and Structural Biotechnology. This is an open access article under the CC BY-NC-ND license (http://creativecommons.org/licenses/by-nc-nd/4.0/).

1. Introduction

The global antimicrobial resistance (AMR) crisis is one of the three biggest threats to human health, as highlighted by the World Health Organization (WHO) [1]. The frequency of infections caused by AMR has increased every year for the past twenty years [2], and has been estimated to be responsible for at least 35,000 deaths annually across the United States [3]. Despite the profound clinical and economic consequences caused by AMR, only few new classes of antibiotics have been approved for clinical use in the past four decades [4]. The diminishing antibiotic pipeline, coupled with the mounting AMR, threatens the modern healthcare system, hence novel therapies are urgently needed to combat infections caused by these 'superbugs' in this rapidly approaching post-antibiotic era. Gram-negative pathogens like *Klebsiella pneumoniae, Acinetobacter baumannii,* and *Pseudomonas aeruginosa* are responsible for the increasing number of nosocomial infections that are difficult to treat as they have accumulated resistance to several classes of antibiotics [5].

---

* Corresponding author.
  E-mail address: tony.velkov@unimelb.edu.au (T. Velkov).

K. pneumoniae is an opportunistic Gram-negative pathogen that is increasingly responsible for both hospital-acquired and community-acquired infections, such as pneumonia, urinary tract infections, and bacteraemia in immunocompromised patients [6–8]. This pathogen can acquire and amplify wider range of AMR genes with increased capability to act like a reservoir for resistance plasmids, which can be trafficked to other Gram-negative pathogens [9]. In fact, many of the common antibiotic-resistant genes found in MDR Gram-negative bacteria were first discovered in the *Klebsiella* species [10].

The emergence of MDR bacteria, combined with the dry antibiotic pipeline, led to the revival of polymyxins as a last-line therapeutic treatment [11]. Polymyxins are an old class of cyclic lipopeptide antibiotics that were approved in the late 1950s [12,13]. Polymyxins have a narrow spectrum of antibacterial activity and are mainly effective against Gram-negative pathogens [14]. The precise mechanisms of action of polymyxins have not yet been fully elucidated, but many theories have been put forth such as the 'self-promoted' uptake mechanism [15,16]. In this putative mechanism, polymyxins are thought to primarily target the lipid A acyl chains on the lipopolysaccharides (LPS) on the outer membrane (OM) of Gram-negative bacteria, resulting in the competitive displacement of ionic bridges that stabilise the LPS and thereby disrupting the OM permeability [13,17,18]. Reports of hetero-resistance in MDR *K. pneumoniae* is suggestive of the inadequacy of polymyxin monotherapy [19]. This has emphasized the urgent need for optimizing of polymyxin exposure for preserving its antimicrobial activity to minimise or limit the further emergence of polymyxin-resistant *K. pneumoniae*. Higher polymyxin B doses and longer duration of therapy are associated with increased prevalence of polymyxin B nephrotoxicity. Hence there is increasing interest in designing effective treatment strategies to treat MDR Gram-negative bacterial infections that limit the polymyxin B exposure, i.e. by polymyxin combination with FDA-approved non-antibiotics [20–22]. The ability of polymyxins to disrupt the OM raises the potential that polymyxins could aid in enabling non-antibiotic drugs to gain entry into the bacteria and interact with the intracellular targets and reveal their antibacterial effects [23–25].

Caspofungin, is one such FDA approved non-antibiotic, a derivative of pneumocandin B0, is a naturally occurring lipophilic cyclic antifungal peptide that belongs to the family of echinocandin [26]. Like polymyxins, caspofungin is reserved for difficult-to-treat invasive fungal infections which occur in immunocompromised patients such as those with malignancies or HIV infections [27,28]. Caspofungin is generally very well tolerated with a highly favourable safety profile due to few adverse effects, limited toxicity and relatively few drug-drug interaction [29,30]. Due to its low toxicity and low resistance rates, caspofungin is a very attractive alternative in fungal infection prophylaxis and treatment [31].

The synergistic bacterial killing activity of polymyxin B plus caspofungin combination treatment has not been studied. Adams et. al (2016) is the only other study that studied the *in vitro* synergistic activity of the polymyxin B-caspofungin combination against fluconazole-resistant *Candida glabrata* yeast isolates [32]. The objective of the present study was to evaluate the potential pharmacodynamics of polymyxins in combination with caspofungin against polymyxin-susceptible and -resistant *K. pneumoniae* isolates and investigate the underlying mechanism of their synergistic activity employing metabolomics and transcriptomics.

2. Results and discussion

2.1. MIC and FICI determination

Polymyxin B and caspofungin MIC results are documented in Supplementary Table S1. Polymyxin B in combination with caspo-

fungin displayed excellent synergy against thirteen polymyxin-susceptible *K. pneumoniae* isolates with FICI values ranging from 0.03 to 0.25. The combination also displayed synergistic activity against three polymyxin-resistant *K. pneumoniae* isolates, including FADDI-KP030, FADDI-KP001 and FADDI-KP005 with FICI values of 0.03, 0.09 and 0.31, respectively. However, indifferent effect (FICI = 0.53) against only one polymyxin-resistant *K. pneumoniae* FADDI-KP062 was seen after combination treatment. Furthermore, the combination did not result in synergistic activity against the other three polymyxin resistant *K. pneumoniae* isolates. This suggests that polymyxin B potentially permeabilizes the polymyxin-susceptible *K. pneumoniae* outer membrane which in turn enables the entry of caspofungin intracellularly and thereby, both drugs work collaboratively to kill the bacteria (Supplementary Table S1) [23,33].

2.2. Time-kill kinetics

Caspofungin as monotherapy against both *K. pneumoniae* strains (*K. pneumoniae* ATCC13883 and FADDI-KP001) exhibited no remarkable antibacterial activity across all time points (Supplementary Fig. S1A and B). While polymyxin B monotherapy (0.25 mg/L) resulted in a significant decrease in bacterial count of *K. pneumoniae* ATCC13883 (>3 $\log_{10}$ CFU/mL) and FADDI-KP001 (>2 $\log_{10}$ CFU/mL) compared to the untreated control by 1 h, however; this was followed by regrowth similar to the control after 4 h (Supplementary Fig. S1A and B).

On the other hand, against the polymyxin-susceptible *K. pneumoniae* ATCC13883, combination therapy was more effective in the first 1 h resulting in > 4 log10 CFU/mL decrease in the initial inoculum, with regrowth suppressed until at least 4 h prior to observable regrowth by 24 h (Supplementary Fig. S1A). A similar trend was observed against the polymyxin-resistant *K. pneumoniae* FADDI-KP001, where the combination of polymyxin B and caspofungin reduced the bacterial inoculum by $\geq$ 3 $\log_{10}$ CFU/mL by 1 h as compared to both the control (untreated) as well as the polymyxin B monotherapy (Supplementary Fig. S1B). The difference in bacterial killing after 1 h between the combination and the polymyxin B monotherapy was much more pronounced for the *K. pneumoniae* FADDI-KP001 (2.3-fold log10 CFU/mL) compared to that for *K. pneumoniae* ATCC 13883 (1.5-fold log10 CFU/mL). Notably, the polymyxin B-caspofungin combination was substantially more effective compared to both monotherapies and control across all time points.

2.3. Metabolic perturbations of K. pneumoniae FADDI-KP001 in response to polymyxin B and caspofungin either alone or as a combination

The killing activity of polymyxin B-caspofungin combination in static time-kill studies was carried out against *K. pneumoniae* FADDI-KP001 ($\sim10^8$ CFU/mL) for the purposes of determining appropriate conditions for sample preparation to perform metabolomics analysis. The polymyxin B concentration of 2 mg/L and caspofungin concentration of 10 mg/L were used as monotherapy and in combination (Supplementary Fig. S2).

Multivariate data analysis using One-way Analysis of Variance (ANOVA) followed by principal component analysis (PCA) were performed in order to determine the significant metabolites affected by treatment conditions ($\geq$0.59-$\log_2$-fold; $p \leq 0.05$). The PCA plots showed that combination treatment samples were significantly separated from all other treatment conditions at 0.5 h (Supplementary Fig. S3A). There was noticeable overlap between the combination treatment and polymyxin B monotherapy at 1 h, suggesting that the combination effect was mainly driven by polymyxin B (Supplementary Fig. S3A). Notably, at the 4 h timepoint

there was some overlap between the polymyxin B and caspofungin mono and the combination treated samples in some components, the combination treatment was still distant from the control (untreated) samples (Supplementary Fig. S3A). Similarly, in line with the previous results, heatmap showed that the impact of combination treatment was significantly different compared to the control and monotherapy with either drug (Supplementary Fig. S3B).

The bacterial metabolome was impacted the most by the combination, perturbing 131, 153 and 162 significant metabolites at 0.5, 1 and 4 h, respectively (Supplementary Fig. S4A). Perturbations produced by monotherapy with either caspofungin and polymyxin B was less comparatively as caspofungin induced only 8 (0.5 h), 14 (1 h) and 10 (4 h) significantly perturbed metabolites while even fewer significant metabolites 14 (0.5 h), 9 (1 h) and 3 (4 h) were induced by polymyxin B (Supplementary Fig. S4A). Notably, there were 117, 135 and 153 unique metabolites induced only by combination therapy at 0.5, 1 and 4 h, respectively (Supplementary Fig. S4B). The combination therapy shared more metabolites with polymyxin B alone (11 intermediates) than with caspofungin (4 metabolites) at 0.5 h; however, at later time points (1 and 4 h) the combination therapy shared more intermediates with caspofungin (12 metabolites, 1 h; 8 metabolites, 4 h) compared to polymyxin B alone (9 metabolites, 1 h; 3 metabolites, 4 h).

The classification of significantly changed metabolites has shown that carbohydrates, amino acids, lipids, nucleotides, and peptides were largely altered compared to other classes of metabolites in response to treatment across all time exposures (0.5, 1 and 4 h) (Supplementary Fig. S5). The highest number of metabolites were altered in response to the combination as compared to monotherapy with polymyxin B and caspofungin. The most significant changes in response to combination treatment were a decrease in carbohydrates (0.5 and 1 h) and amino acids (4 h) while an elevation in the abundance of lipids was seen across all time points (0.5, 1 and 4 h) (Supplementary Fig. S5).

2.4. Transcriptomics analysis of K. pneumoniae FADDI-KP001 treated with polymyxin B, caspofungin and their combination

Transcriptomics study was employed to investigate the transcriptomic responses of *K. pneumoniae* FADDI-KP001 following treatment with mono and combination treatment with polymyxin B (2 mg/L) and caspofungin (10 mg/L) at 0.5, 1 and 4 h. At 0.5 h, a total of 349/190 (up/down) and 98/80 (up/down) differentially expressed genes (DEGs) were induced by monotherapy with polymyxin B and caspofungin respectively. Transcriptomic response observed following treatment with polymyxin B-caspofungin resulted in 474/394 (up/down) DEGs at 0.5 h (≥ 1.0-log$_2$-fold, $p \leq 0.05$) (Supplementary Fig. S6A). DEGs at 1 h following monotherapy with polymyxin B (89 up/94 down) and caspofungin (26 up/17 down) were lower compared to the number of DEGs (148 up/343 down) expressed in response to the combination treatment (≥ 1.0-log$_2$-fold, $p \leq 0.05$). Similarly, at 4 h, mono- and combination therapy with polymyxin B and caspofungin resulted in 84/26 (up/down), 102/45 (up/down) and 290/96 (up/down) DEGs (≥ 1.0-log$_2$-fold, $p \leq 0.05$) respectively (Supplementary Fig. S9A). Across all time points, venn diagrams generated from the RNA expression profiles revealed polymyxin B as the main driver of perturbations in gene expression in the polymyxin B-caspofungin combination treatment. There were a large number of differentially expressed genes in common between polymyxin B and combination, particularly at 0.5 h (209 DEGs) and 1 h (49 DEGs) (Supplementary Fig. S6B). The number of unique DEGs in the combination treatment were 254 (0.5 h), 92 (1 h) and 174 (4 h) (Supplementary Fig. S6B). DEGs of each time point (0.5, 1 and 4 h) following each treatment (polymyxin B, caspofungin and the combination) were mapped to the metabolic pathways.

Similar to the metabolomic analysis, the polymyxin B-caspofungin combination treatment comparatively affected significantly more pathways compared to either monotherapy. Intriguingly, cell envelope biogenesis, PTS, ABC transporter system, central carbon metabolism and fatty acid biosynthesis were among the most significantly expressed pathways across all time points. The genes names and annotation of the DEGs involved in the significantly expressed pathways are listed in Supplementary Table S2.

2.5. Metabolic analyses of perturbations in lipid metabolism

Monotherapy with either polymyxin B or caspofungin had no effect on lipid intermediates of *K. pneumoniae* FADDI-KP001, and all perturbations in lipid metabolism were caused by combination therapy only across the earlier time points of 0.5, 1 and 4 h (Fig. 1). The crucial precursors of bacterial membrane lipids, *sn*-glycero-3-phosphoethanolamine (log$_2$FC = 3.08) and *sn*-glycero-3-phosphocholine (log$_2$FC = 3.02) were significantly increased following combination therapy at 0.5 h (Fig. 1). However, CDP-dipalmitoyl-*sn*-glycerol, a CDP-diacyl-glycerol that functions as a biosynthetic intermediate in the formation of the major membrane-forming phospholipid phosphatidylcholine [34], was extensively reduced (log$_2$FC = -7.93) due to the combination treatment at 0.5 h. Polymyxin B-caspofungin caused nearly equal perturbations in fatty acids and glycerophospholipids metabolites at 0.5 h. However, the combination treatment induced a different response at 1 h, wherein the impact on the levels of fatty acid intermediates (10 metabolites) were higher compared to the shift in glycerophospholipids (only 3 metabolites) (Fig. 1). At 1 h, two essential membrane phospholipid fatty acids, namely FA(16:0) (log$_2$FC = 3.15) and FA(17:0) (log$_2$FC = 3.51) were significantly increased in response to the combination treatment (Fig. 1). It is hypothesized that increased abundance of these saturated fatty acids can decrease the fluidity of the bacterial membrane which in turn will reduce the LpxK activity and thereby, biogenesis of LPS [35,36]. At 4 h, the combination induced more perturbations in fatty acids compared to glycerophospholipids, including membrane phospholipid fatty acid FA(16:0), FA hydroxy(16:0) and FA oxo(16:0) (≥ 1.5-log$_2$-fold; $p \leq 0.05$). (Fig. 1).

2.6. Analyses of metabolic and transcriptomic changes in cell wall biosynthesis and interconnected pathways

One of the main antibiotic targets in bacteria is the bacterial cell wall and OM. It has been shown that one of the possible bacterial killing mechanisms displayed by polymyxins is the disorganisation and destabilisation of the bacterial OM [12,37]. Diaminopimelic acid (DAP) is an amino acid that is utilised as an intermediate for lysine biosynthesis as well as DAP-type peptidoglycan formation in several Gram-negative bacteria [38]. A high level of suppression in the abundance of multiple key metabolites involved in cell wall biosynthesis (amino- and nucleotide sugar metabolism, lysine, peptidoglycan and LPS biosynthetic pathways) was clearly observed after polymyxin B-caspofungin treatment particularly at 1 h (Fig. 2A & B). At 0.5 h, the level of few building blocks of cell wall envelope were significantly reduced after polymyxin B-caspofungin treatment (Supplementary Fig. S7). However, more perturbation due to the combination therapy occurred at 1 h, at which the combination therapy caused a significant suppression in the levels of three key precursors of amino- and nucleotide sugar metabolism [1,6-anhydro-*N*-acetylmuramate, *N*-acetylmuramate and UDP-*N*-acetylmuramate] and the intimately interrelated LPS biogenesis pathway [D-ribose 5-phosphate, D-sedoheptulose 7-phosphate and 3-deoxy-D-*manno*-octulosonate (KDO)] (≥ -1.0-log$_2$-fold, $p \leq 0.05$) (Fig. 2A & B). Admittedly, D-sedoheptulose 7-
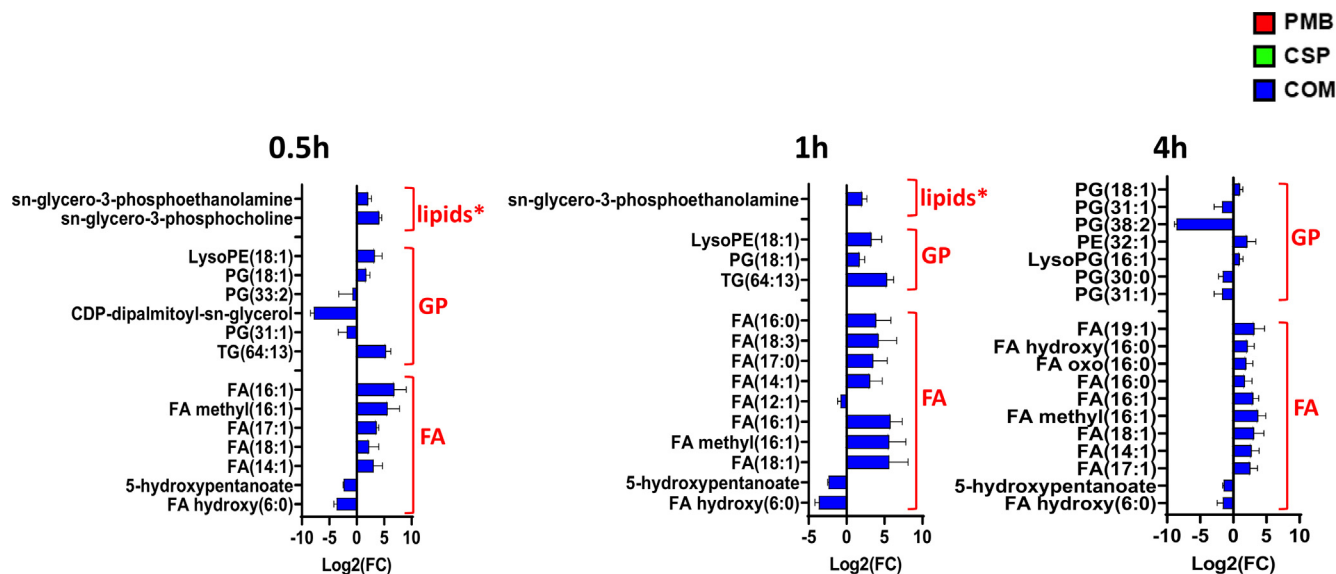
Fig. 1. Significantly perturbed lipids in *K. pneumoniae* FADDI-KP001 following treatment with polymyxin B (PMB, red), caspofungin (CSP, green) and their combination (COM, blue) at 0.5, 1 and 4 h. Lipid names are putatively assigned based on accurate mass (≥ 0.59-$\log_2$-fold, $p \leq 0.05$). * Lipids other than fatty acids and glycerophospholipids. PE, phosphoethanolamines; PG, glycerophosphoglycerols; LysoPG, lysoglycerophospholipids; TG, triacylglycerol; FA, fatty acids. (For interpretation of the references to colour in this figure legend, the reader is referred to the web version of this article.)
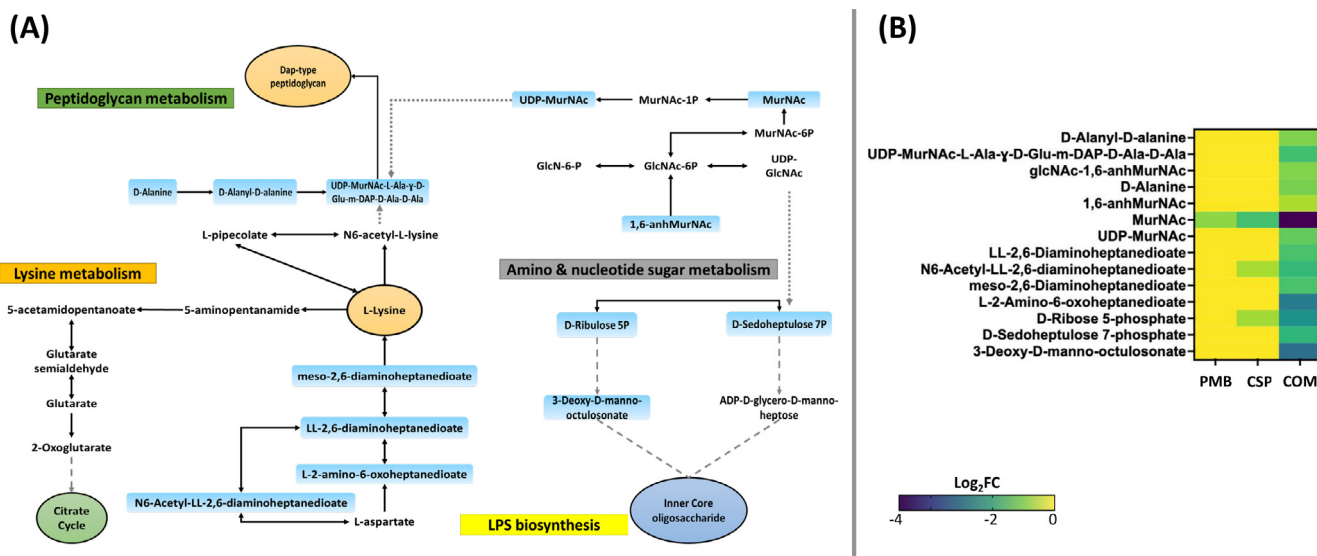

Fig. 2. (A) Diagrammatic and (B) heatmap representation of all significantly impacted metabolites involved in the interconnected pathways of the cell envelope biogenesis (amino- and nucleotide sugar metabolism, lysine, peptidoglycan, and lipopolysaccharide (LPS) biosynthetic pathways) in *K. pneumoniae* FADDI-KP001 after polymyxin B (PMB) and caspofungin (CSP) monotherapies and their combination (COM) at 1 h ($\geq$-1.0-$\log_2$-fold, $p \leq 0.05$). Blue rectangles represent the downregulated metabolites. (For interpretation of the references to colour in this figure legend, the reader is referred to the web version of this article.)

phosphate is a heptose unit that makes up one of the key building blocks of the LPS inner core of Gram-negative bacteria as well as act as a central metabolite for the pentose phosphate pathway; KDO is highly conserved in bacteria and is essential for cell viability [39]. Furthermore, another downstream pathways, peptidoglycan, and lysine metabolisms, were significantly perturbed in response to polymyxin B-caspofungin combination therapy at 1 h (Fig. 2A & B).

In comparison to 0.5 and 1 h, the combination therapy caused more perturbations in the lysine pathway than other cell wall formation interconnected pathways such as amino- and nucleotide sugar metabolism, peptidoglycan and LPS pathways at 4 h, wherein the abundance of ten intermediates of lysine pathway were signif-

icantly supressed (except for 5-aminopentanamide, $\log_2$FC = 2.05), namely LL-2,6-diaminoheptanedioate, N6-acetyl-LL-2,6-diamino heptanedioate, *meso*-2,6-diaminoheptanedioate, N6-acetyl-L-lysine, L-pipecolate, 5-acetamidopentanoate, 5-aminopentanoate, 2-oxoglutarate and glutarate ($\geq$-1.0-$\log_2$-fold, $p \leq 0.05$) (Supplementary Fig. S7). Notably, both polymyxin B and caspofungin monotherapies displayed minor impact on all cell wall interconnected pathways (lysine, amino- and nucleotide sugar metabolism, peptidoglycan and LPS pathways) at all time exposure (0.5, 1 and 4 h) (Fig. 2B; Supplementary Fig. S7).

In line with the metabolomics results, the combination treatment resulted in more genes involved in metabolic pathways (amino- and nucleotide sugar metabolism, lysine, peptidoglycan

and LPS biosynthetic pathways) related to the cell wall assembly at all time points, particularly 1 h (Fig. 3A-C). While polymyxin B and caspofungin alone resulted in minimal changes in DEGs of these pathways at 0.5, 1 and 4 h (Fig. 3A-C). Intriguingly, a marked rise in the expression of a crucial gene *ftsI*, which involved in the catalysis of cross-linking of the peptidoglycan cell wall [40], was observed following polymyxin B alone and the combination treatment at 0.5 and 1 h ($\geq$1.0-log$_2$-fold, $p \leq 0.05$) (Fig. 3C). Furthermore, at the same time exposure 0.5 and 1 h, both polymyxin B monotherapy and the combination therapy caused a significant up-regulation in LPS inner core formation gene namely *kdsC* ($\geq$1.0-log$_2$-fold, $p \leq 0.05$) (Fig. 3C) [41]. Importantly, a gene (*lpxD*) coding for the lipid A biosynthesis, a phosphorylated glycolipid that moors the LPS with the bacterial outer membrane, was up regulated in response to caspofungin monotherapy (log$_2$FC = 1.25) and the combination therapy (log$_2$FC = 1.25) at 1 h (Fig. 3C) [42]. At 4 h, all treatment groups induced less perturbation in genes involved in the interconnected metabolic pathways of the cell envelope formation (Fig. 3A-C).

2.7. Metabolic and transcriptomic alteration of the central carbon metabolism

Central carbohydrate metabolism in bacteria is a complex cellular network which involves multiple pathways such as glycolysis, pentose phosphate pathway (PPP), citrate cycle and tricarboxylic acid cycle (TCA) and hence the target of investigation for a new generation of antibiotics [43,44]. Pathway enrichment analysis revealed that polymyxin B-caspofungin treatment induced a greater perturbation in metabolites involved in central carbon metabolism across all time points (0.5, 1 and 4 h) while minor changes in these pathways were caused by polymyxin B and caspofungin treatment alone (Fig. 4; Supplementary Fig. S8). Polymyxin B-caspofungin therapy resulted in a significant decline in the levels of eight fundamental building blocks of glycolysis pathway at 0.5 h, whereas the abundance of only two essential elements of the glycolysis were significantly reduced following treatment with polymyxin B alone (Supplementary Fig. S8A). Furthermore, the levels of crucial precursors of the closely related pathways the PPP (acetyl-CoA, (S)-lactate, *cis*-aconitate, succinate and citrate) and the TCA cycle (D-sedoheptulose 7-phosphate and 6-phospho-2-dehydro-D-gluconate) were significantly perturbed following the combination therapy at 0.5 h (Supplementary Fig. S8A). Polymyxin B monotherapy also reduced the abundance of acetyl-CoA (log$_2$-FC = -0.61) at 0.5 h (Supplementary Fig. S8A). It is a well-known that acetyl-CoA mediates several metabolic processes in bacteria such as supply of acetyl groups to citrate cycle, fatty acid and amino acid biosynthesis, and it is mainly supplied by the glycolysis [45].

At 1 h, polymyxin B monotherapy had no impact on central carbon metabolism, whereas caspofungin monotherapy significantly suppressed the levels of three key metabolites (D-fructose 1,6-bisphosphate, D-glyceraldehyde 3-phosphate and glycerone phosphate) from glycolysis and one key component (D-ribose 5-phosphate) from PPP at 1 h ($\geq$-1.0-log$_2$-fold, $p \leq 0.05$) (Fig. 4). This perturbation paled in comparison to the impact of polymyxin B-caspofungin combination treatment, where twenty metabolites in central carbon metabolism pathway, including 9 glycolysis ntermediates (e.g., glycerone phosphate and D-glucose), 6 TCA intermediates (e.g., succinate and citrate) and 5 PPP intermediates (e.g., D-ribose-5-phosphate and D-sedoheptulose-7-phospahte), were markedly declined ($\geq$-1.0-log$_2$-fold, $p \leq 0.05$) (Fig. 4). The TCA cycle has a direct role in bacterial cellular respiration, as well as supplies several key metabolites, such as succinate and citrate, which are important intermediates required for other bacterial metabolic processes such as fatty acid and amino acid metabolism [46]. The effect of the combination treatment on glycolysis, PPP and TCA started to decline at 4 h, which was comparable to its effect at
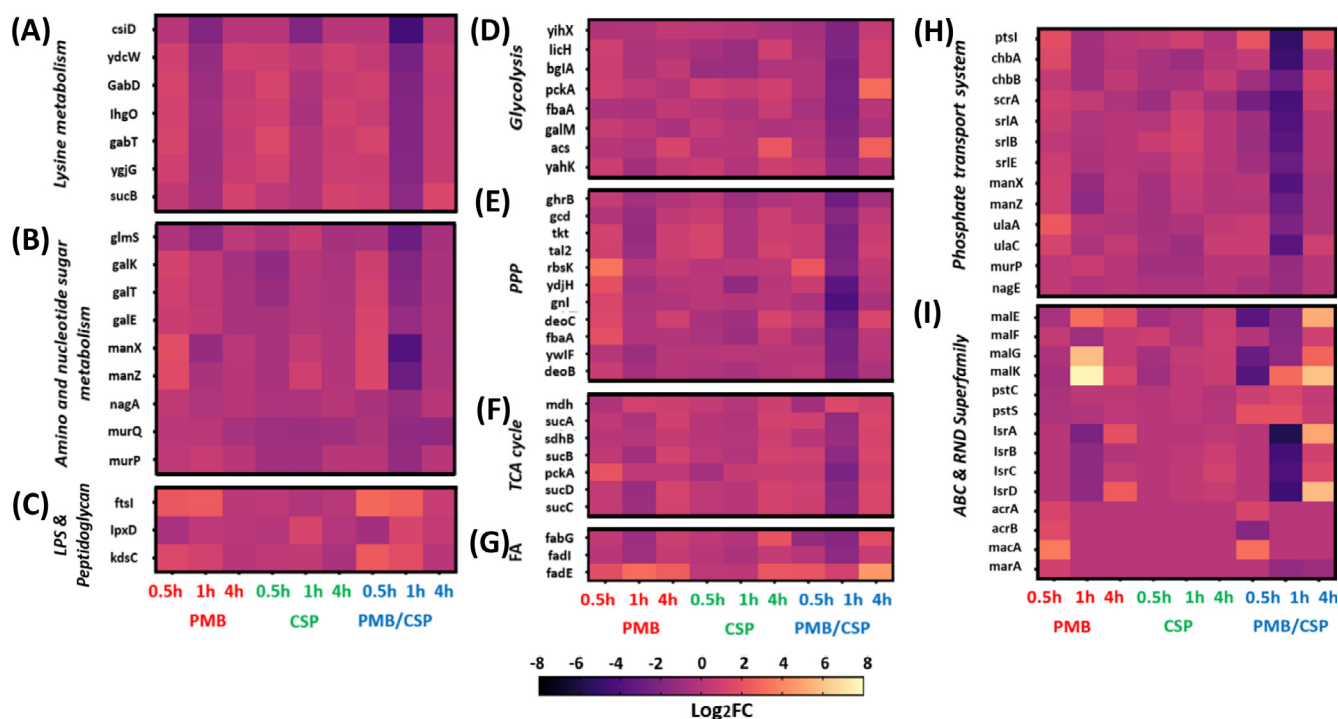

Fig. 3. Differentially expressed genes (log$_2$ fold change) of *K. pneumoniae* FADD-KP001 after polymyxin B (PMB), caspofungin (CSP) and the combination (PMB/CSP) treatments involved in the cell wall biosynthesis interconnected pathways of amino- and nucleotide sugar metabolism, lysine, peptidoglycan and lipopolysaccharide biosynthetic pathways, and phosphotransferase system, ABC transporter and RND operon, glycolysis, pentose phosphate pathway, citrate cycle and fatty acids metabolic pathways at 0.5, 1 and 4 h (>1.0-log$_2$-fold, $p \leq 0.05$).
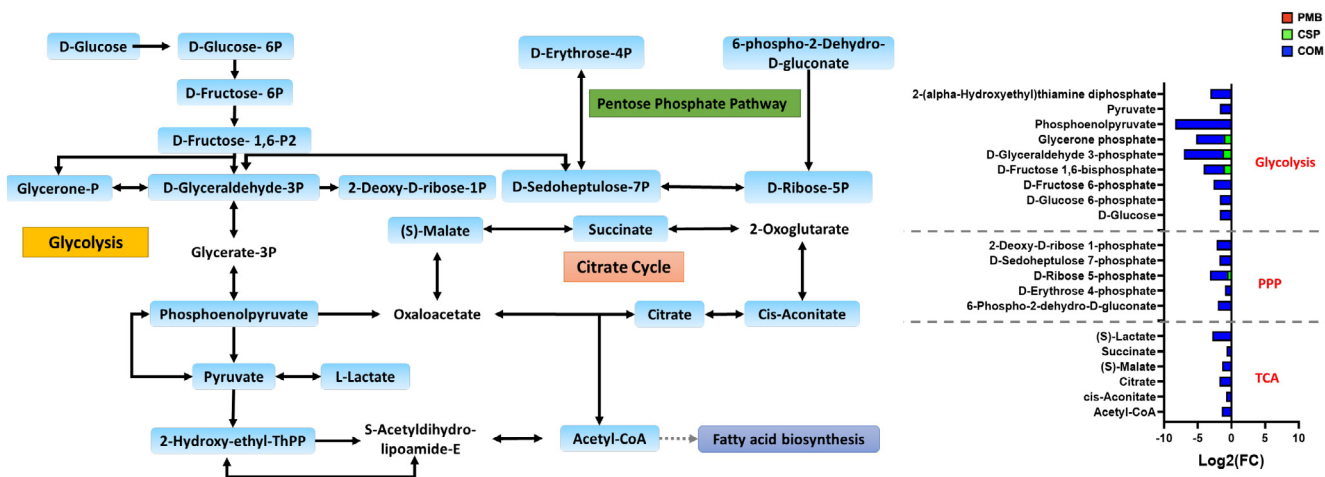
Fig. 4. Schematic pathway diagram depicting the significantly influenced precursors of central carbon metabolism (glycolysis, pentose phosphate pathway, citrate cycle) and interrelated fatty acid biosynthetic pathway of *K. pneumoniae* FADDI-KP001 due to polymyxin B (PMB), caspofungin (CSP) monotherapies and their combination at 1 h ($\geq$-1.0-log$_2$-fold, $p \leq 0.05$). Blue rectangles represent the supressed metabolites. (For interpretation of the references to colour in this figure legend, the reader is referred to the web version of this article.)

0.5 h (Supplementary Fig. S8B). In comparison to the combination treatment, polymyxin B and caspofungin monotherapies did not display significant impact on the central carbon metabolism at 4 h (Supplementary Fig. S8B).

The transcriptomic response of central carbon metabolism (glycolysis, PPP, and TCA) was similar to patterns of abovementioned metabolic pathways, where polymyxin B-caspofungin combination caused extensive dysregulation in the levels of genes involved in this complex pathway across all time points, in particular 1 h (Fig. 3D-F). While polymyxin B and caspofungin monotherapies induced expression of central carbon metabolism genes at 0.5, 1 and 4 h to a lesser extent (Fig. 3D-F). In glycolysis, polymyxin B (4 h) and the combination therapy (1 and 4 h) significantly dysregulated the expression of an essential gene namely *acs* ($\geq$1.0-log$_2$-fold, $p \leq 0.05$) (Fig. 3D). Interestingly, *acs* gene, encoding acetyl-coenzyme A synthetase, can mediate the conversion of acetate into acetyl-CoA, the latter is an essential intermediate used by bacterial cell to generate energy via TCA cycle and helps maintain the bacterial cell membrane integrity via formation of fatty acid precursors [47,48]. Notably, polymyxin B and caspofungin *per se* caused a significant upregulation in the abundance of principal TCA cycle gene *sucA* at 4 h ($\geq$1.0-log$_2$-fold, $p \leq 0.05$) (Fig. 3F). Whereas the expression of *sucA* was significantly supressed following polymyxin B-caspofungin therapy at 1 h ($\geq$-1.0-log$_2$-fold, $p \leq 0.05$); nevertheless, at 4 h, the combination therapy revealed a conversed pattern as indicated by causing a significant upregulation in the level of the same gene ($\geq$1.0-log$_2$-fold, $p \leq 0.05$) (Fig. 3E). It has been found that *sucA* gene knockout attenuates TCA cycle and glycolysis in Gram-negative bacteria, which in turn impairs the proton motive force and bacterial cell growth [49].

2.8. Metabolic and transcriptomic perturbations of the fatty acid biosynthesis

Phospholipids in bacterial OM is made up of glycerolipids with two fatty acid chains. These acyl chains determine membrane viscosity, which in turn has an influence on many key membrane-associated bacterial functions, namely membrane permeability for hydrophobic molecules (including drugs), active transport and protein–protein interactions [50]. Therefore, survival is highly dependent on membrane lipid homeostasis and the ability of bacteria to adjust their lipid composition in response to their external environments [51]. As a result, fatty acid biosynthesis pathway has

been studied as a novel target for antibacterial drug discovery [52]. Fatty acid biosynthesis is closely related pathway to the central carbon metabolism [53].

Intriguingly, polymyxin B-caspofungin treatment significantly disorganised the fatty acids biosynthesis pathway at all time exposure particularly 1 h (Supplementary Fig. S9). Whilst polymyxin B and caspofungin treatment alone had no impact on fatty acid biosynthesis at all time points (0.5, 1 and 4 h) (Supplementary Fig. S9). Notably, a significant rise in the levels of three essential fatty acids components (tetradecanoic acid, (9Z)-hexadecenoic acid and (9Z)-octadecenoic acid) was observed following the combination treatment at 0.5 and 4 h ($\geq$1.5-log$_2$-fold, $p \leq 0.05$) (Supplementary Fig. S9). However, a greater impact was induced by polymyxin B-caspofungin treatment at 1 h, wherein the levels of five metabolites namely tetradecanoic acid, octadecanoic acid, dodecanoic acid, (9Z)-hexadecenoic acid and (9Z)-octadecenoic acid were significantly increased ($\geq$1.0-log$_2$-fold, $p \leq 0.05$) (Supplementary Fig. S9).

In the transcriptomic analysis, polymyxin B and caspofungin monotherapies significantly dysregulated a fundamental transcript of fatty acid metabolism namely *fabG* at 1 and 4 h, respectively ($\geq$1.0-log$_2$-fold, $p \leq 0.05$) (Fig. 3G). Similarly, *fabG* experienced a marked downregulation with polymyxin B in combination with caspofungin at 0.5 and 1 h (log$_2$FC = -1.30 and −1.84, respectively), which at the later time point 4 h conversely displayed an overrepresentation (log$_2$FC = 1.77) (Fig. 3G). Furthermore, the level of *fadI* gene was significantly downregulated (log$_2$FC = -1.59) in response to polymyxin B-caspofungin combination treatment at 1 h (Fig. 3G). The *fabG* and *fadI* genes play an important role in the synthesis of fatty acids in Gram-negative bacteria as they are required for the elongation of saturated and unsaturated fatty acid [53]. Downregulation of long-chain fatty acid transport protein (FadL) is associated with antimicrobial peptides resistant Gram-negative bacteria; therefore, there has been a growing interest to develop antibacterial agents to target fatty acid biosynthesis [54,55].

2.9. Metabolic and transcriptomic perturbations in phosphotransferase system (PTS) pathway

PTS in Gram-negative bacteria, plays various roles in multiple aspects of bacterial physiology such as biofilm formation, virulence, and transposon-mediated directed mutation [56–58]. It also plays a role in the catalysis of sugar transport, phosphorylation and

chemoreception, in addition to these primary functions, it possesses secondary functions like metabolic and transcriptomic regulations [59]. Apart from its potential impact on membrane structure, pathway enrichment analysis also illustrated that the effect of the combination therapy on PTS pathway was prominent at 1 h (12 metabolites) compared to the minor impact it had at 0.5 h (5 metabolites) and 4 h (4 metabolites). On the other hand, polymyxin B and caspofungin monotherapies, in comparison to the combination treatment, caused a minor effect on the PTS pathway at 0.5, 1 and 4 h (Fig. 5; Supplementary Fig. S10).

Notably, the polymyxin B-caspofungin combination produced extensive reduction in the abundance of crucial precursor of PTS pathway phosphoenolpyruvate (PEP) largely at 1 h ($log_2FC = -8.3$) and to a lesser extent at 4 h ($log_2FC = -0.94$) (Fig. 5). PEP is used by PTS as the main energy source for the uptake of metabolites as well as a phosphoryl donor for phosphorylation [60]. Therefore, such a pronounced reduction in PEP levels would undoubtedly undermine the primary and secondary metabolic functions of PTS as well as the control of various physiological processes.

Our transcriptomics data showed that all detected genes encoding for PTS pathway following polymyxin B-caspofungin treatment were remarkably downregulated at 1 h, which was increasingly prominent compared to monotherapy with either drug at the same time point ($\geq$-1.0-log_2-fold, $p \leq 0.05$) (Fig. 3H). The impact of all treatment groups on the levels of gene expression involved in PTS pathway at 0.5 and 4 h were less pronounced compared to 1 h. Notably, the expression of two essential PTS genes (*ptsI* and *murP*) underwent a significant decline following the combination therapy at 1 h ($\geq$-1.0-log_2-fold, $p \leq 0.05$) (Fig. 3H). It was revealed that the deletion of *ptsI* gene from PTS of Gram-negative bacteria associated with inability of bacteria to utilise carbon sources, reduced its invasion, and lowered its virulence [61]. Intriguingly, *murP* gene, encoding PTS system *N*-acetylmuramic acid-specific EIIBC component, is essential as it helps to transport

N-acetylmuramic acid (MurNAc) across bacterial cell membrane, which forms with *N*-acetylglucosamine (GlcNAc) the backbone of the cell wall peptidoglycan of both Gram-positive and Gram-negative bacteria [62].

2.10. Metabolic and transcriptomic perturbations of the multidrug efflux pumps [ABC transporters and resistance-nodulation-division (RND) transporters]

The ABC and RND superfamilies are most important multidrug transporters in Gram-negative bacteria that have a very diverse range of functions, ranging from importing essential nutrients in bacteria to multi-drug resistance [63–65]. They have been exploited recently as druggable targets for development of antibacterial agents [66,67]. There has been a marked perturbation in the metabolites of ABC transporter pathway following polymyxin B-caspofungin treatment at all the time points, 0.5, 1 and 4 h, comparing to no significant impact by either drug alone (Supplementary Table S3). At 0.5 h, only four metabolites (orthophosphate, L-valine, L-glutamine and glutathione) were markedly suppressed following combination treatment ($\geq$-1.0-log_2-fold, $p \leq 0.05$) (Supplementary Table S3). The combination induced a pronounced reduction in ten key metabolites of ABC transporter at 1 h, including orthophosphate, L-ornithine, L-valine, L-glutamate, L-glutamine, L-histidine, betaine, glutathione, maltose and mannitol ($\geq$-1.0-log_2-fold, $p \leq 0.05$) (Supplementary Table S3). In comparison, fewer key metabolite levels were significantly affected at 4h, only half the number of metabolites, five metabolites, namely orthophosphate, L-valine, betaine, glutathione and L-proline ($\geq$-1.0-log_2-fold, $p \leq 0.05$) were suppressed due to treatment with the combination (Supplementary Table S3).

A similar pattern was seen in transcriptomics data wherein polymyxin B-caspofungin combination therapy induced a significant alteration in the expression of genes involved in the bacterial
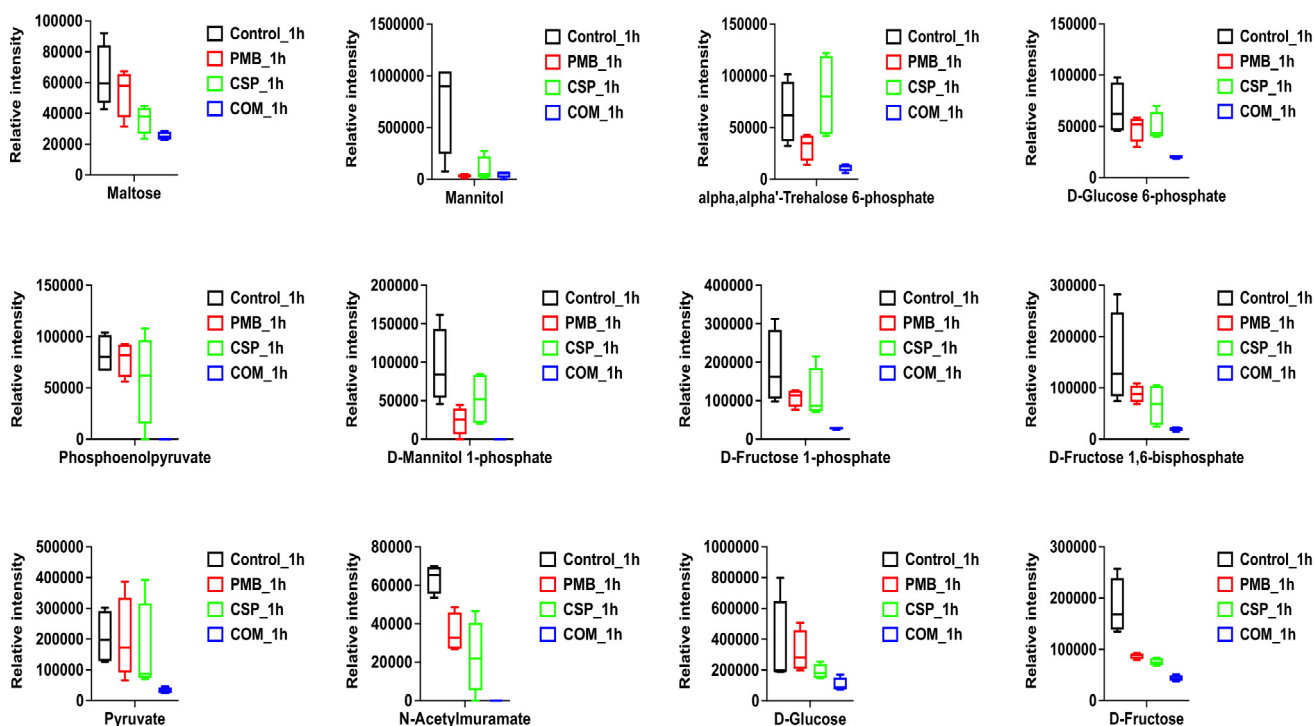

Fig. 5. Whisker plots of significantly impacted metabolites of phosphotransferase system (PTS) pathway in *K. pneumoniae* FADDI-KP001 following polymyxin B (PMB) and caspofungin (PMB) monotherapies and polymyxin B-caspofungin combination (COM) treatment at 1 h ($\geq$-1.0-log_2-fold, $p \leq 0.05$).

drug efflux pumps [ABC transporter system and the resistance-nodulation-cell division (RND) superfamily] at all time exposures (0.5, 1 and 4 h), more pronounced at 1 h (Fig. 3I). Polymyxin B monotherapy induced minor perturbation of ABC transporter system genes at 0.5 h; however, this transcriptomic response intensified at 1 h and to a lesser extent at 4 h (Fig. 3I). No significant influence (except for *isrD*, $log_2FC = 1.06$ at 4 h) on ABC transporter and RND operon genes was recognized following caspofungin monotherapy at all time points 0.5, 1 and 4 h (Fig. 3I). Importantly, the expressions of essential genes namely *macA* ($log_2FC = 3.57$), a regulator of MacAB–TolC multidrug efflux pumps [68], and *marA* gene ($log_2FC = 1.02$, a modulator of the multiple antibiotic resistance (mar) operon in Gram-negative bacteria [69], were significantly upregulated in response to polymyxin monotherapy at 0.5 h (Fig. 3I)[68]. Furthermore, polymyxin B treatment alone increased the level of two crucial genes (*acrA*, $log_2FC = 1.34$ and *acrB*, $log_2FC = 1.62$) involved in the regulating of AcrAB–TolC (RND-based multidrug efflux pumps) at the same time point (0.5 h) (Fig. 3I)[64]. Similarly, but to a certain limit, polymyxin B-caspofungin combination caused a significant upregulation in the level of *acrA* and *macA* ($log_2FC = 1.27$ and 3.17, respectively), and downregulation in the expression of *acrB* ($log_2FC = -1.87$) at 0.5 h (Fig. 3I). In contrast to polymyxin B monotherapy effect on *marA* gene, polymyxin B-caspofungin combination caused a significant decrease in the expression of *marA* gene at 1 and 4 h, $log_2FC = -1.35$ and -1.05, respectively (Fig. 3I). It has been reported that a repression in *marA* gene leads to the reduced expression of the AcrAB-TolC efflux pump, and hence a decreased resistance to multiple antibiotics such as polymyxins [70,71]. Furthermore, it has been reported that the inactivation of the efflux pump AcrAB in *E. coli* evolved a phenotype with an 8-fold increase in colistin antibiotic sensitivity [72].

3. Conclusions

Our multi-omics study is the first to investigate the antibacterial killing synergy of polymyxins and caspofungin against *K. pneumoniae*. Combination of polymyxins with caspofungin at clinically relevant concentrations demonstrated synergistic antibacterial killing and multiple interrelated metabolic pathways involved in the synergistic killing activity were revealed, including cell envelope assembly, central carbon metabolism, fatty acid biosynthesis, phosphotransferase system and ATP-binding cassette (ABC) transporter. Notably, remarkable reduction in metabolites and gene expression levels in almost all affected pathways specifically at 1 h. We purport a synergistic killing mechanism wherein polymyxins initially disrupt the bacterial outer membrane that in turn enables the entry of caspofungin, which then exerts its action intracellularly against the aforementioned pathways. Overall, this project underlines the potential of repurposing the FDA approved caspofungin against *K. pneumoniae*. This will ultimately aid in the clinical translation and help preserve the activity of last-line polymyxins for the treatment of multidrug-resistant infections.

4. Methods

4.1. Bacterial strains

Twenty different *K. pneumoniae* isolates, including 13 polymyxin-susceptible and 7 polymyxin-resistant isolates were employed in this study (Supplementary Table S1). All strains (except for ATCC 13883 and ATCC 70072) were obtained from Women's and Children's Hospital (Adelaide, SA, Australia) [73]. The antibiogram of the clinical isolate *K. pneumoniae* FADDI-KP001 is documented in Supplementary Table S4. The European

Committee on Antimicrobial Susceptibility Testing (EUCAST) clinical breakpoints for polymyxin B for Enterobacteriaceae (e.g., *K. pneumoniae*) are as a susceptible breakpoint of ≤ 2 mg/L and a resistant breakpoint > 2 mg/L [74]. All isolates were stored in tryptone soy broth (Oxoid) with 20% glycerol (Ajax Finechem, Seven Hills, NSW, Australia) in cryovials at −80 °C. The strains were sub-cultured onto nutrient rich agar plates (Media Preparation Unit, University of Melbourne, Melbourne, VIC, Australia) and incubated at 37 °C for 24 h prior to use.

4.2. Antibiotics and reagents

Cation-Adjusted Mueller-Hinton broth (Oxoid, England) supplemented with calcium and magnesium (CAMHB; 25.0 mg/L Ca^{2+}, 12.5 mg/L Mg^{2+}) was used for susceptibility testing and in vitro experiments. Stock solutions of polymyxin B (Beta Pharma, China, Batch number 20120204) solutions were prepared in Milli-Q™ water (Millipore, Australia). Stock solutions of caspofungin (Selleckchem, USA, Batch number S3073) were prepared using dimethyl sulfoxide (DMSO; Sigma-Aldrich, Australia). All drug solutions were filter sterilized by using a 0.22-µm filter (Sartorius, Australia). All other reagents were purchased from Sigma-Aldrich (Australia) and were of the highest commercial grade available.

4.3. Determination of MIC and FICI

The minimum inhibitory concentrations (MICs) for polymyxin B and caspofungin were determined in triplicates using by broth microdilution method [75]. Checkerboard experimental setup was used to determine the activity of polymyxin B in combination with caspofungin against a panel of eight *K. pneumoniae* strains (4 polymyxin-susceptible strains and 4 polymyxin-resistant strains). The interactive effect between the two drugs was determined by calculating the fractional inhibitory concentration index (FICI) using the equation below

$$FICI = \frac{MICofDrugAincombination}{MICofDrugA} + \frac{MICofDrugBincombination}{MICofDrugB} \qquad (1)$$

FICI of ≤ 0.5 is indicative of synergy, FICI = 1 indicates additivity while FICI > 1 and < 4 indicates indifference, while FICI ≥ 4 indicates antagonism [76]. All tested strains were exposed to a final concentration of DMSO (2.5%, v/v) which had no inhibitory effect on their growth. All experiments were carried out in triplicates.

4.4. Time-kill assay

Briefly, as previously described static time–kill experiments were conducted to characterise the pharmacodynamic activity of polymyxin B (0.25 mg/L) and caspofungin (10 mg/L) as mono- and in combination against an initial inoculum of 10^6 CFU/mL over 24 h incubated in shaking water bath at 37 °C (shaking speed, 150 rpm) [77]. The mean maximum tolerated plasma concentrations of caspofungin in human following a single dose of 70, 100 and 150 mg, administered intravenously are 14.2, 20.3 and 30.4 mg/L respectively [78,79]. Therefore, the selected caspofungin concentration (10 mg/L) in this study is representative of a clinically achievable plasma concentration. Static time-kill analysis was performed against two *K. pneumoniae* isolates (ATCC 13883, polymyxin B MIC = 0.5 mg/L; and FADDI-KP001, polymyxin B MIC = 4 mg/L) that were selected based on their FICI values. Serial cultures were obtained at 0, 0.5, 1, 4 and 24 h. Bacterial counts were determined based on quantitative cultures on Mueller–Hin-

ton agar plates after 24 h of incubation at 37 °C. All experiments were performed in triplicates.

5. Metabolomics

5.1. Bacterial culture preparation for metabolomics

An untargeted metabolomic study was conducted to investigate the underlying mechanisms of synergy of polymyxin B and caspofungin against polymyxin resistant *K. pneumoniae* isolate FADDI-KP001. Logarithmic phase broth culture was prepared prior to each experiment by adding fresh *K. pneumoniae* FADDI-KP001 colonies from overnight growth to pre-warmed CAMHB (37 °C) to achieve the desired initial inoculum of $\sim 10^8$ CFU/mL ($OD_{600} \sim 0.5$). Polymyxin B and caspofungin as mono- or in combination were added to the logarithmic phase bacterial culture to achieve the appropriate polymyxin B (2 mg/L) and caspofungin (10 mg/L) concentrations. The higher starting inoculum was used to prevent excessive bacterial killing. Each 200 mL culture was incubated at 37 °C in Bioline rotary shaker (shaking speed 180 rpm) and 15 mL samples were withdrawn from each treatment group at 0.5, 1, and 4 h. The OD_{600} for each sample was measured and normalized to ~ 0.5 with fresh CAMHB. The samples were quenched and centrifuged at $3,220 \times g$ at 4C for 15 min. Lastly, the supernatants were discarded, and the pellets were stored at -80 °C, for further metabolite extraction. The experiment was conducted in four biological replicates to minimise the bias from inherent random variation.

5.2. Metabolite extraction

The bacterial pellets were washed twice in 1 mL of 0.9% NaCl followed by centrifugation at $3220 \times g$ at 4C for 5 min to remove residual extracellular metabolites. Chloroform:methanol: water (1:3:1 v/v/v) extraction solvent containing 1 μM each of the internal standards (CHAPS, CAPS, PIPES and TRIS) was added to the resuspended pellets. The internal standards selected are physiochemically diverse small molecules that are not found naturally occurring in any microorganism. Samples were then frozen thrice in liquid nitrogen, thawed on ice and then vortexed to release the intracellular metabolites. After the third cycle, samples were centrifuged again for 10 min at $3220 \times g$ at 4C, wherein the supernatants were transferred into 1.5 mL Eppendorf tubes to be stored immediately at -80C. Prior to analysis, samples must be thawed and centrifuged at $14,000 \times g$ at 4C for 10 min to remove any particulate matter, and then 200 μL of sample was transferred into the injection vial for LC-MS analysis. An equal volume of each sample was combined to be used as a quality control sample so that a sample will contain all analytes during the analysis [80].

5.3. LC-MS analysis

Hydrophilic interaction liquid chromatography (HILIC) - high-resolution mass spectrometry using a Dionex high-performance liquid chromatography system (RSLCU3000, Thermo Fisher) with a ZIC-PHILIC column (5 μm, polymeric, 150 × 4.6 mm; SeQuant, Merck) was employed for identifying polar metabolites. The system was linked to a Q-Exactive Orbitrap mass spectrometer (Thermo Fisher) equipped with positive and negative electrospray (ESI) modes at 35,000 resolutions with a mass range of 85 to 1,275 *m/z*. The LC solvents were (A) 20 mM ammonium carbonate and (B) acetonitrile, operated via a multi-step gradient system. The gradient system started at 80% B and was decreased to 50% B over 15 min, then reduced from 50% B to 5% B over 3 min, thereafter washed with 5% B for another 3 min, and finally 8 min re-

equilibration with 80% B at a flow rate of 0.3 mL/min [81]. The cycle time was 32 min with an injection sample volume of 10 μL. To avoid batch-to-batch variation, all samples were analysed as a single LC-MS batch. A mixture containing over 250 metabolites used as pure standards, were processed as a part of the analysis batch to help with metabolite identification.

5.4. Data processing, bioinformatics, and statistical analyses

Raw mass spectrometry data was processed by IDEOM (http://mzmatch.sourceforge.net/ideom.php) [82] employing ProteoWizard to convert the raw LC-MS data into a .mzXML format. XCMS is freely available software package used for raw peak detection, while Mzmatch.R, is a software package developed to extend the capabilities of XCMS [83,84] for aligning the samples, as well as for filtering peaks by using a minimum peak intensity threshold of 100,000 with a relative standard deviation (RSD) of <0.5 (reproducibility), and peak shape (codadw) of >0.8. Mzmatch.R was also used to retrieve any missing peaks and annotate related peaks. Unwanted noise and artefact peaks were removed using default IDEOM parameters. While loss of a proton was corrected in negative ESI mode, the gain of a proton was corrected in positive ESI mode, followed by identification of metabolites based on their exact mass within 2 ppm. The identification of each metabolite (Level 1 identification based on MSI standards) was confirmed using the retention rates of authentic standards. Other metabolites were identified (Level 2 identification based on MSI standards) using exact mass and predicted retention time based on the Kyoto Encyclopedia of Genes and Genomes (KEGG; http://www.genome.jp/kegg/), MetaCyc, and LIPIDMAPS databases. In cases where isomers could not be clearly differentiated by retention time, preference to bacterial metabolites annotated in EcoCyc was used. MetaboAnalyst 5.0, a free online tool used for performing statistical analysis (https://www.metaboanalyst.ca). Putative metabolites with median RSD ≤ 0.2 (20%) within the QC group and IDEOM confidence level of ≥ 5 were incorporated into a table and then uploaded to MetaboAnalyst. Half of the minimum positive values in the original data will be used to replace features with >25% missing values. The interquartile range were used to filter the data and then $\log_2$ transformation and auto scaling were preformed to normalise the data. One-way ANOVA ($p < 0.05$ for Fisher's LSD; fold change threshold = 2) was used to identify metabolites with significant changes control and treatment groups. KEGG mapper was used to build the metabolic pathway modules by uploading the KEGG IDs of the statistically significant metabolites.

5.5. RNA extraction and analysis of RNA sequencing data

A 1.5 mL from each sample (polymyxin B 2 mg/L, caspofungin 10 mg/L as mono- and in combination) were collected at 0.5, 1 and 4 h for RNA extraction. The RNA was extracted according to the RNeasy Mini Kit manufacturer's protocol (Qiagen, Germany). Libraries were prepared with the Nextera library preparation kit, using a protocol previously described. RNA-seq of 36 samples in total were sequenced using Illumina HiSeq 1500 at Genewiz (paired-end 150 bp, Illumina HiSeq, Suzhou, China). The raw reads were aligned to the strain genome by Rsubread v2.6.3. The counts of mapped reads were summarised by featureCounts. Differential gene expressions were identified using voom and limma linear modeling methods via a web-based RNA-seq visualization software Degust (http://degust.erc.monash.edu), a graphic interface [85]. Statistical significance of differential gene expression (DEG) is defined using a cut-off of ≥ 1.0-$\log_2$-fold and FDR ≤ 0.05. PCA plots and venn diagrams were generated using MetaboAnalyst 5.0 (https://www.metaboanalyst.ca) and GeneVenn, respectively [86]. Gene ontology and pathway enrichment analysis of DEGs

were performed using biochemical databases of KEGG (http://www.genome.jp/kegg/) and BioCyc (https://biocyc.org/).

CRediT authorship contribution statement

Maytham Hussein: Conceptualization, Data curation, Formal analysis, Investigation, Methodology, Software, Writing – original draft, Writing – review & editing. **Labell J.M. Wong:** Data curation, Investigation, Software, Writing – review & editing. **Jinxin Zhao:** Data curation. **Vanessa E. Rees:** Data curation, Writing – review & editing. **Rafah Allobawi:** Writing – review & editing. **Rajnikant Sharma:** Resources, Writing – review & editing. **Gauri G. Rao:** Resources, Validation, Writing – review & editing. **Mark Baker:** Resources, Writing – review & editing. **Jian Li:** Funding acquisition, Validation, Writing – review & editing. **Tony Velkov:** Funding acquisition, Supervision, Validation, Writing – review & editing.

Declaration of Competing Interest

Appendix A. Supplementary data

Supplementary data to this article can be found online at https://doi.org/10.1016/j.csbj.2022.02.021.

References

[1] The 10 x '20 Initiative: pursuing a global commitment to develop 10 new antibacterial drugs by 2020. Clinical infectious diseases : an official publication of the Infectious Diseases Society of America. 2010;50:1081-3.
[2] Ejaz H, Wang N, Wilksch JJ, Page AJ, Cao H, Gujaran S, et al. Phylogenetic analysis of Klebsiella pneumoniae from hospitalized children, Pakistan. Emerg Infectious Diseases 2017;23:1872.
[3] CDC. Antibiotic resistance threats in the United States, 2019.Atlanta, GA: U.S. Department of Health and Human Services, CDC;2019. 2019.
[4] Butler MS, Paterson DL. Antibiotics in the clinical pipeline in October 2019. J Antibiotics 2020;73:329–64.
[5] Ejaz H, Younas S, Qamar MU, Junaid K, Abdalla AE, Abosalif KOA, et al. Molecular epidemiology of extensively drug-resistant mcr encoded colistin-resistant bacterial strains co-expressing multifarious β-lactamases. Antibiotics 2021;10:467.
[6] Montgomerie John Z. Epidemiology of Klebsiella and hospital-associated infections. Rev Infect Dis 1979;736.
[7] Seo JH, Hong JS, Kim D, Cho BK, Huang TW, Tsai SF, et al. Multiple-omic data analysis of Klebsiella pneumoniae MGH 78578 reveals its transcriptional architecture and regulatory features. BMC Genomics 2012;13:679.
[8] Paczosa MK, Mecsas J. Klebsiella pneumoniae: going on the offense with a strong defense. Microbiol Mol Biol Rev 2016;80:629–61.
[9] Wyres KL, Holt KE. Klebsiella pneumoniae as a key trafficker of drug resistance genes from environmental to clinically important bacteria. Curr Opin Microbiol. 2018;45:131–9.
[10] Bengoechea JA, Sa Pessoa J. Klebsiella pneumoniae infection biology: living to counteract host defences. FEMS Microbiol Rev. 2019;43:123–44.
[11] Falagas ME, Kasiakou SK. Colistin: the revival of polymyxins for the management of multidrug-resistant gram-negative bacterial infections. Clin Infect Dis 2005;40:1333–41.
[12] Velkov T, Roberts KD, Nation RL, Thompson PE, Li J. Pharmacology of polymyxins: new insights into an 'old' class of antibiotics. Future Microbiol 2013;8:711–24.
[13] Peleg AY, Hooper DC. Hospital-acquired infections due to gram-negative bacteria. New Engl J Med 2010;362:1804–13.
[14] Arnold TM, Forrest GN, Messmer KJ. Polymyxin antibiotics for gram-negative infections. Am J Health-system Pharmacy 2007;64:819–26.
[15] Nation RL, Li J, Cars O, Couet W, Dudley MN, Kaye KS, et al. Framework for optimisation of the clinical use of colistin and polymyxin B: the Prato polymyxin consensus. Lancet Infect Dis 2015;15:225–34.
[16] Velkov T, Roberts KD, Nation RL, Thompson PE, Li J. Pharmacology of polymyxins: new insights into an 'old'class of antibiotics. Future Microbiol 2013;8:711–24.
[17] Velkov T, Thompson PE, Nation RL, Li J. Structure–activity relationships of polymyxin antibiotics. J Med Chem 2010;53:1898–916.
[18] Zavascki AP, Goldani LZ, Li J, Nation RL. Polymyxin B for the treatment of multidrug-resistant pathogens: a critical review. J Antimicrobial Chemotherapy 2007;60:1206–15.
[19] Poudyal A, Howden BP, Bell JM, Gao W, Owen RJ, Turnidge JD, et al. In vitro pharmacodynamics of colistin against multidrug-resistant Klebsiella pneumoniae. J Antimicrob Chemother. 2008;62:1311–8.
[20] Hussein M, Schneider-Futschik EK, Paulin OK, Allobawi K, Crawford S, Zhou QT, et al. Effective strategy targeting polymyxin-resistant gram-negative pathogens: polymyxin B in combination with the selective serotonin reuptake inhibitor sertraline. ACS Infect Dis 2020;6:1436–50.
[21] Hussein M, Hu X, Paulin OK, Crawford S, Zhou QT, Baker M, et al. Polymyxin B combinations with FDA-approved non-antibiotic phenothiazine drugs targeting multi-drug resistance of Gram-negative pathogens. Comput Struct Biotechnol J 2020;18:2247–58.
[22] Krishnamurthy M, Lemmon MM, Falcinelli EM, Sandy RA, Dootz JN, Mott TM, et al. Enhancing the antibacterial activity of polymyxins using a nonantibiotic drug. Infection and Drug Resistance 2019;12:1393.
[23] Hussein MH, Schneider EK, Elliott AG, Han M, Reyes-Ortega F, Morris F, et al. From breast cancer to antimicrobial: combating extremely resistant Gram-negative "superbugs" using novel combinations of polymyxin B with selective estrogen receptor modulators. Microbial Drug Resistance 2017;23:640–50.
[24] Betts JW, Sharili AS, La Ragione RM, Wareham DW. In vitro antibacterial activity of curcumin–polymyxin B combinations against multidrug-resistant bacteria associated with traumatic wound infections. J Nat Prod 2016;79:1702–6.
[25] Tran TB, Bergen PJ, Creek DJ, Velkov T, Li J. Synergistic killing of polymyxin B in combination with the antineoplastic drug mitotane against polymyxin-susceptible and-resistant Acinetobacter baumannii: a metabolomic study. Front Pharmacol 2018;9:359.
[26] McCormack PL, Perry CM. Caspofungin. Drugs 2005;65:2049–68.
[27] Singh N. Trends in the epidemiology of opportunistic fungal infections: predisposing factors and the impact of antimicrobial use practices. Clin Infectious 2001;33:1692–6.
[28] Pfaller MA, Diekema DJ. Epidemiology of invasive candidiasis: a persistent public health problem. Clin Microbiol Rev 2007;20:133–63.
[29] Sable C, Nguyen BYT, Chodakewitz J, DiNubile M. Safety and tolerability of caspofungin acetate in the treatment of fungal infections. Transplant Infectious Disease 2002;4:25–30.
[30] Stone JA, Holland SD, Wickersham PJ, Sterrett A, Schwartz M, Bonfiglio C, et al. Single-and multiple-dose pharmacokinetics of caspofungin in healthy men. Antimicrob Agents Chemother 2002;46:739–45.
[31] Rosanova MT, Bes D, Serrano Aguilar P, Cuellar Pompa L, Sberna N, Lede R. Efficacy and safety of caspofungin in children: systematic review and meta-analysis. Archivos argentinos de pediatria. 2016;114:305–12.
[32] Adams EK, Ashcraft DS, Pankey GA. In vitro synergistic activity of caspofungin plus polymyxin B against fluconazole-resistant Candida glabrata. Am J Med Sci 2016;351:265–70.
[33] Allison DG, Lambert PA. Modes of action of antibacterial agents. Molecular Medical Microbiology: Elsevier; 2015. p. 583-98.
[34] Geiger O, López-Lara IM, Sohlenkamp C. Phosphatidylcholine biosynthesis and function in bacteria. Biochim Biophys Acta (BBA)-Mol Cell Biol Lipids 2013;1831:503–13.
[35] Emiola A, Andrews SS, Heller C, George J. Crosstalk between the lipopolysaccharide and phospholipid pathways during outer membrane biogenesis in Escherichia coli. Proc Natl Acad Sci 2016;113:3108–13.
[36] Zhang Y-M, Rock CO. Membrane lipid homeostasis in bacteria. Nat Rev Microbiol 2008;6:222–33.
[37] Hancock RE, Chapple DS. Peptide antibiotics. Antimicrobial Agents and Chemotherapy 1999;43:1317–23.
[38] Barton D, Meth-Cohn O. Comprehensive natural products chemistry. Newnes 1999.
[39] Taylor PL, Blakely KM, de Leon GP, Walker JR, McArthur F, Evdokimova E, et al. Structure and function of sedoheptulose-7-phosphate isomerase, a critical enzyme for lipopolysaccharide biosynthesis and a target for antibiotic adjuvants. J Biol Chem 2008;283:2835–45.
[40] Weiss DS, Pogliano K, Carson M, Guzman LM, Fraipont C, Nguyen-Distèche M, et al. Localization of the Escherichia coli cell division protein FtsI (PBP3) to the division site and cell pole. Mol Microbiol 1997;25:671–81.
[41] Martorana AM, Sperandeo P, Polissi A, Dehò G. Complex transcriptional organization regulates an Escherichia coli locus implicated in lipopolysaccharide biogenesis. Res Microbiol 2011;162:470–82.
[42] Bartling CM, Raetz CR. Crystal structure and acyl chain selectivity of Escherichia coli LpxD, the N-acyltransferase of lipid A biosynthesis. Biochemistry 2009;48:8672–83.
[43] Noor E, Eden E, Milo R, Alon U. Central carbon metabolism as a minimal biochemical walk between precursors for biomass and energy. Mol Cell 2010;39:809–20.
[44] Murima P, McKinney JD, Pethe K. Targeting bacterial central metabolism for drug development. Chem Biol 2014;21:1423–32.
[45] Wolfe A. Glycolysis for microbiome generation. Microbiol Spectr 2015. https://doi.org/10.1128/microbiolspec. MBP-0014-2014.
[46] Gest H. Evolutionary roots of the citric acid cycle in prokaryotes. Biochem Soc Symp. 1987;54:3–16.
[47] Brown T, Jones-Mortimer M, Kornberg H. The enzymic interconversion of acetate and acetyl-coenzyme A in Escherichia coli. Microbiology 1977;102:327–36.

[48] Polyak SW, Abell A, Wilce MCJ, Zhang L, Booker GW. Structure, function and selective inhibition of bacterial acetyl-coa carboxylase. Appl Microbiol Biotechnol 2012;93:983–92.

[49] Li M, Ho PY, Yao S, Shimizu K. Effect of sucA or sucC gene knockout on the metabolism in Escherichia coli based on gene expressions, enzyme activities, intracellular metabolite concentrations and metabolic fluxes by 13C-labeling experiments. Biochem Eng J 2006;30:286–96.

[50] Parsons JB, Rock CO. Is bacterial fatty acid synthesis a valid target for antibacterial drug discovery? Curr Opin Microbiol. 2011;14:544–9.

[51] Zhang YM, Rock CO. Membrane lipid homeostasis in bacteria. Nat Rev Microbiol. 2008;6:222–33.

[52] Campbell JW, Cronan Jr JE. Bacterial fatty acid biosynthesis: targets for antibacterial drug discovery. Annual Rev Microbiol 2001;55:305–32.

[53] Heath RJ, Rock CO. Enoyl-acyl carrier protein reductase (fabI) plays a determinant role in completing cycles of fatty acid elongation in Escherichia coli (∗). J Biol Chem 1995;270:26538–42.

[54] Heath RJ, Rock CO. Fatty acid biosynthesis as a target for novel antibacterials. Current opinion in investigational drugs (London, England: 2000). 2004;5:146.

[55] Shen CJ, Kuo TY, Lin CC, Chow LP, Chen WJ. Proteomic identification of membrane proteins regulating antimicrobial peptide resistance in Vibrio parahaemolyticus. J Appl Microbiol 2010;108:1398–407.

[56] Barabote RD, Saier Jr MH. Comparative genomic analyses of the bacterial phosphotransferase system. Microbiol Mol Biol Rev: MMBR 2005;69:608–34.

[57] Le Bouguénec C, Schouler C. Sugar metabolism, an additional virulence factor in enterobacteria. Int J Med Microbiol 2011;301:1–6.

[58] Lopes MS, Gosset G, Rocha RC, Gomez JG, Ferreira da Silva L. PHB biosynthesis in catabolite repression mutant of Burkholderia sacchari. Curr Microbiol 2011;63:319–26.

[59] Kundig W, Ghosh S, Roseman S. Phosphate bound to histidine in a protein as an intermediate in a novel phospho-transferase system. Proc Natl Acad Sci U S A. 1964;52:1067–74.

[60] Deutscher J, Aké FMD, Derkaoui M, Zébré AC, Cao TN, Bouraoui H, et al. The bacterial phosphoenolpyruvate: carbohydrate phosphotransferase system: regulation by protein phosphorylation and phosphorylation-dependent protein-protein interactions. Microbiol Mol Biol Rev 2014;78:231–56.

[61] Zhi Y, Lin SM, Ahn KB, Ji HJ, Guo HC, Ryu S, et al. ptsI gene in the phosphotransferase system is a potential target for developing a live attenuated Salmonella vaccine. Int J Mol Med 2020;45:1327–40.

[62] Dahl U, Jaeger T, Nguyen BT, Sattler JM, Mayer C. Identification of a phosphotransferase system of Escherichia coli required for growth on N-acetylmuramic acid. J Bacteriol 2004;186:2385–92.

[63] Davidson AL, Dassa E, Orelle C, Chen J. Structure, function, and evolution of bacterial ATP-binding cassette systems. Microbiol Mol Biol Rev 2008;72:317–64.

[64] Du D, Wang-Kan X, Neuberger A, van Veen HW, Pos KM, Piddock LJ, et al. Multidrug efflux pumps: structure, function and regulation. Nat Rev Microbiol 2018;16:523–39.

[65] Fernando DM, Kumar A. Resistance-nodulation-division multidrug efflux pumps in gram-negative bacteria: role in virulence. Antibiotics 2013;2:163–81.

[66] Garmory HS, Titball RW. ATP-binding cassette transporters are targets for the development of antibacterial vaccines and therapies. Infect Immun 2004;72:6757–63.

[67] Venter H, Mowla R, Ohene-Agyei T, Ma S. RND-type drug efflux pumps from Gram-negative bacteria: molecular mechanism and inhibition. Front Microbiol 2015;6:377.

[68] Lu S, Zgurskaya HI. MacA, a periplasmic membrane fusion protein of the macrolide transporter MacAB-TolC, binds lipopolysaccharide core specifically and with high affinity. J Bacteriol 2013;195:4865–72.

[69] Sharma P, Haycocks JR, Middlemiss AD, Kettles RA, Sellars LE, Ricci V, et al. The multiple antibiotic resistance operon of enteric bacteria controls DNA repair and outer membrane integrity. Nat Commun 2017;8:1–12.

[70] Lázár V, Martins A, Spohn R, Daruka L, Grézal G, Fekete G, et al. Antibiotic-resistant bacteria show widespread collateral sensitivity to antimicrobial peptides. Nat Microbiol 2018;3:718–31.

[71] Sundaramoorthy NS, Suresh P, Ganesan SS, GaneshPrasad A, Nagarajan S. Restoring colistin sensitivity in colistin-resistant E. coli: combinatorial use of MarR inhibitor with efflux pump inhibitor. Sci Rep 2019;9:1–13.

[72] Gogry FA, Siddiqui MT, Sultan I, Haq QMR. Current update on intrinsic and acquired colistin resistance mechanisms in bacteria. Front Med 2021;8.

[73] Li J, Turnidge J, Milne R, Nation RL, Coulthard K. In vitro pharmacodynamic properties of colistin and colistin methanesulfonate against Pseudomonas aeruginosa isolates from patients with cystic fibrosis. Antimicrob Agents Chemother 2001;45:781–5.

[74] Testing TECoAS. Clinical breakpoints - breakpoints and guidance V.11.0. EUCAST; 2021.

[75] Institute TCaLS. Performance Standards for Antimicrobial Susceptibility Testing. 31 ed. 950 West Valley Road, Suite 2500. Wayne, PA 19087-1898. United States: The Clinical and Laboratory Standards Institute 2021.

[76] Berenbaum MC. What is synergy? Pharmacol Rev 1989;41:93–141.

[77] Rao GG, Ly NS, Diep J, Forrest A, Bulitta JB, Holden PN, et al. Combinatorial pharmacodynamics of polymyxin B and tigecycline against heteroresistant Acinetobacter baumannii. Int J Antimicrob Agents 2016;48:331–6.

[78] Würthwein G, Cornely OA, Trame MN, Vehreschild JJ, Vehreschild MJ, Farowski F, et al. Population pharmacokinetics of escalating doses of caspofungin in a phase II study of patients with invasive aspergillosis. Antimicrob Agents Chemother 2013;57:1664–71.

[79] Cornely O, Vehreschild J, Vehreschild M, Würthwein G, Arenz D, Schwartz S, et al. Phase II dose escalation study of caspofungin for invasive aspergillosis. Antimicrob Agents Chemother 2011;55:5798–803.

[80] Gika HG, Theodoridis GA, Wingate JE, Wilson ID. Within-day reproducibility of an HPLC− MS-based method for metabonomic analysis: application to human urine. J Proteome Res 2007;6:3291–303.

[81] Zhang T, Creek DJ, Barrett MP, Blackburn G, Watson DG. Evaluation of coupling reversed phase, aqueous normal phase, and hydrophilic interaction liquid chromatography with Orbitrap mass spectrometry for metabolomic studies of human urine. Anal Chem 2012;84:1994–2001.

[82] Creek DJ, Jankevics A, Burgess KE, Breitling R, Barrett MP. IDEOM: an Excel interface for analysis of LC-MS-based metabolomics data. Bioinformatics 2012;28:1048–9.

[83] Scheltema RA, Jankevics A, Jansen RC, Swertz MA, Breitling R. PeakML/mzMatch: a file format, Java library, R library, and tool-chain for mass spectrometry data analysis. Anal Chem. 2011;83:2786–93.

[84] Smith CA, Want EJ, O'Maille G, Abagyan R, Siuzdak G. XCMS: processing mass spectrometry data for metabolite profiling using nonlinear peak alignment, matching, and identification. Anal Chem. 2006;78:779–87.

[85] Soneson C, Delorenzi M. A comparison of methods for differential expression analysis of RNA-seq data. BMC Bioinf 2013;14:1–18.

[86] Pirooznia M, Nagarajan V, Deng Y. GeneVenn - A web application for comparing gene lists using Venn diagrams. Bioinformation 2007;1:420–2.